AGENT BASED MONITORING FOR INVESTIGATION PROCESS AND MAINTENANCE IMPROVEMENT

Ameer Hussein Ali, Zouhair I. Ahmed, Soroor K.Hussain

ABSTRACT

Agent technology has a widespread usage in most of computerized systems. In this paper agent technology has been applied to monitor wear test for an aluminium silicon alloy which is used in automotive parts and gears of light loads. In addition to wear test monitoring، porosity effect on wear resistance has been investigated. To get a controlled amount of porosity, the specimens have been made by powder metallurgy process with various pressures (100, 200 and 600) MPa. The aim of this investigation is a proactive step to avoid the failure occurrence by the porosity.

A dry wear tests have been achieved by subjecting three reciprocated loads (1000, 1500 and 2000)g for three periods (10, 45 and 90)min. The weight difference after each test is immediately measured to find the losing weight and wear rate for each specimen. Wear test was monitored online by two sensors, force sensor to control the applied load, find friction force and coefficient of friction. The sensor is an acoustic emission to detect crack initiations of the worn surface by transfers the emitted ultrasonic waves from crack initiations to electric signals. Scanning electron microscope has been used to examine the worn surfaces. The overall results include that the effect of pores depends on pore shapes, sizes and concentrations.

Keywords: Agent Technology, Aluminium Silicon Alloys, Monitoring Process, Acoustic Emission Sensor, Wear, Scanning Electron Microscope and Predictive Maintenance.

الخلاصة:

تقنية العميل لها استخدام واسع في معظم الأنظمة المسيطر عليها بواسطة الحاسوب. في هذا البحث تم تطبيق تكنلوجيا العميل لمراقبة فحص البليان لسبيكة الأمنيوم سليكون التي تدخل في صناعة اجزاء السيارات ومنتجات اخرى كتروس الأحمال الخفيفة. بالاضافة الى مراقبة فحص البلي، تم التحقيق من تأثير المسامية على مقاومة البليان. للحصول على كمية مسيطر عليها من المسامية تم تصنيع العينات بواسطة عملية مساحيق المعادن مع ضغوطات متغيرة (١٠٠، ٢٠٠ و٦٠٠) ميكا باسكال. الهدف من هذا الفحص هو الخطوة الاستباقية لتجنب حدوث الفشل الناتج من المسامية.

اختبارات البلي الجاف قد انجزت عن طريق تسليط ثلاثة احمال تبادلية (١٠٠٠، ١٥٠٠ و٢٠٠٠) غم لثلاث فترات (١٠، ٤٥ و ٩٠) دقيقة. تم قياس الفارق بالوزن مباشرة بعد اختبارات البلي الجاف قد انجزت عن طريق تسليط ثلاثة احمال تبادلية (١٠٠٠، ١٥٠٠ و٢٠٠٠) غم لثلاث فترات (١٠، ٤٥ و ٩٠) دقيقة، وتم قياس الفارق بالوزن مباشرة بعد كل عملية فحص لإيجاد فقدان الوزن ومعدل البلي لكل عينة. اما فحوصات البلي تم مراقبتها بصورة مباشرة بواسطة متحسسين، احدهما متحسس القوى واستخدم لضبط الحمل المسلط ، ايجاد قوة الإحتكاك و معامل الاحتكاك. اما المتحسس الاخر هو متحسس الانبعاثا ت الصوتية لكشف بدايات التصدع في السطح المبلي عن طريق تحويل الموجات فوق الصوتية المنبعثة من بداية التصدع الى اشارة كهربائية. تم استعمال المجهر الماسح الألكتروني لفحص السطوح البالية. تضمنت النتائج بشكل اساس ايجاد تأثير المسامية على مقاومة البليان الذي يعتمد على شكل وحجم وتراكيز المسامات على في المعدن.

1. Introduction:

Agents could be designed to work with uncertain and/or incomplete information and knowledge. Hence, many tasks related to manufacturing - from engineering design to supply chain management - could be conducted by agents, small and large, simple and sophisticated, fine- and coarse-grained that were enabled and empowered to communicate and cooperate with each other [11]. An agent is just something that acts (agent comes from the Latin agere, to do). But computer agents are expected to have other attributes that distinguish them from mere "programs" such as operating under autonomous control, perceiving their environment, persisting over a prolonged time period, adapting to change, and being capable of taking on another's goals[14]. An abstract view of an agent is shown in Fig.1. In this paper agent system is represented by Universal Material Tester machine which is shown in Fig. 2. Sensors are represented by acoustic emission sensor and strain gage which is involved in the load cell while the action is represented by monitoring results of agent environment which is the wear test environment.

Measurement of wear is one of big importance not only in tribology research but also in practical applications, such as engineering surface inspection, coating failure detection, tool wear monitoring and so on. Due to the complexity of a wear analysis process, measurement of wear is usually conducted offline. Reliable online measurement or monitoring of wear remains a challenge to tribology research as well as to the industry [21]. Signals of acoustic emission sensor is useful to detect the level of degradation for the part which is made by type of the alloy which is subjected for the wear test by making comparison between the signals at the work with those come from the wear test. Agent monitoring will give the report of the wear resistance behavior as acoustic emission sensor signals with a description represents by wear track depth data. That report will be the reference to know the state of the product which is made from the same alloy which is used in the test by compare the output signals from that product with the signals of the test by using acoustic emission sensor similar to that which is used in the test.
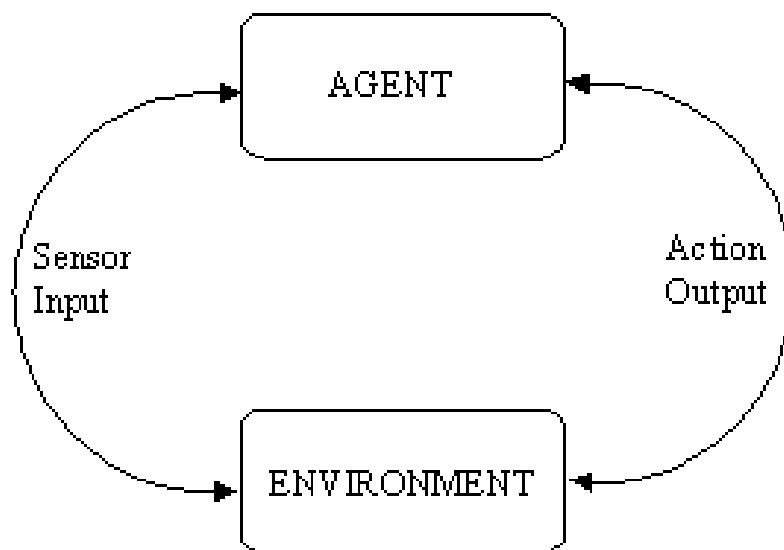

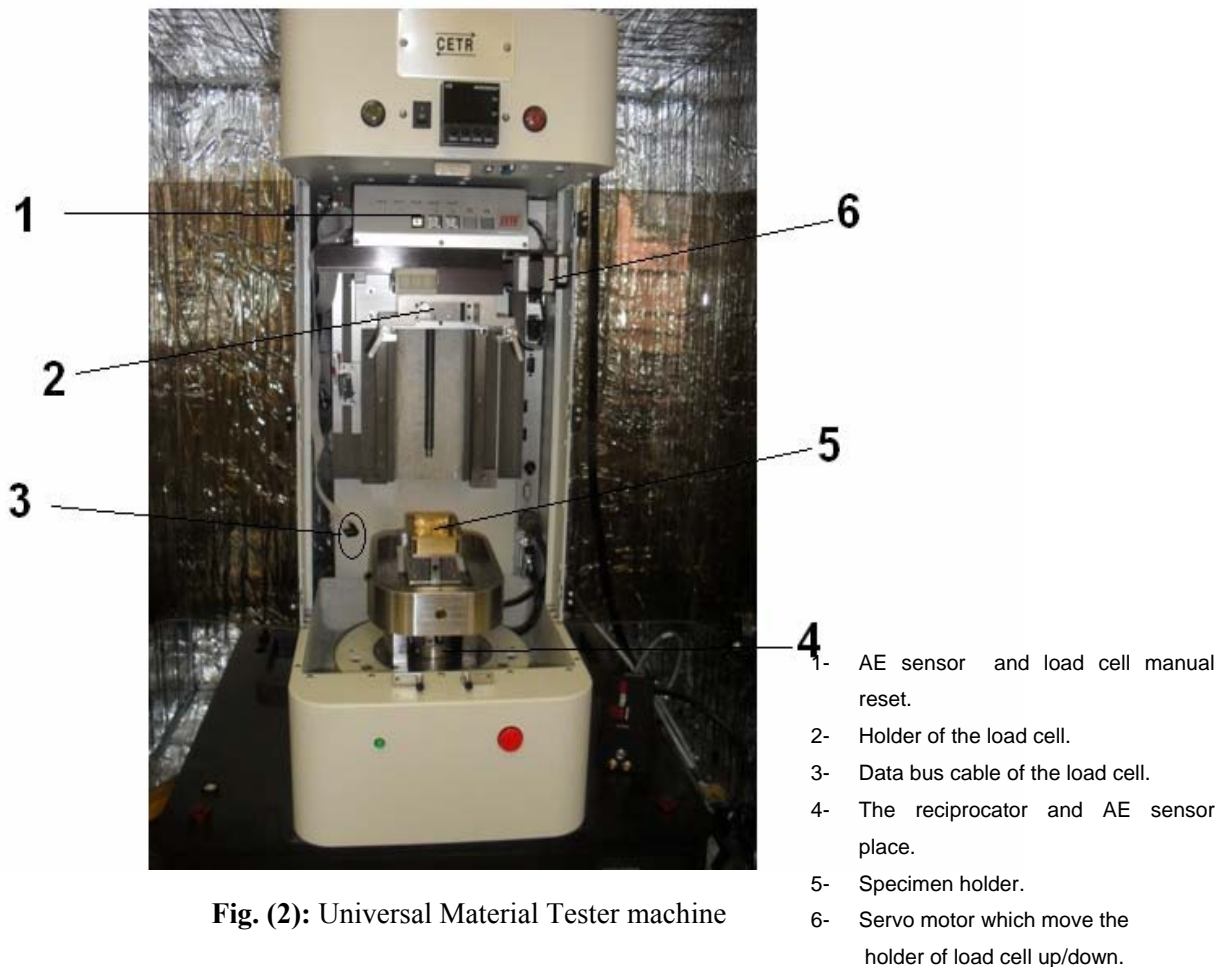**Fig. (1)**: An agent in its environment [5].

Fig. (2): Universal Material Tester machine

1- AE sensor and load cell manual reset.
2- Holder of the load cell.
3- Data bus cable of the load cell.
4- The reciprocator and AE sensor place.
5- Specimen holder.
6- Servo motor which move the holder of load cell up/down.

2. Aluminium Silicon Alloys:

The characteristic property of aluminium alloys is relatively high tensile strength in relation to density compared with that of other cast alloys, such as ductile cast iron or cast steel. The high specific tensile strength of aluminium alloys is very strongly influenced by their composed polyphase microstructure. The silicon content in standardized commercial cast aluminium silicon alloys is in the range of 5 to 23 wt. %. The structure of the alloys can be hypoeutectic, hypereutectic, or eutectic, as can be seen on the equilibrium phase diagram Fig.3. Aluminium–Silicon alloys are a common choice for such applications, and their applicability in gears and structural parts subjected to wear is well established. A higher amount of silicon increases hardness and wear resistance [13] [10]. The alloy which is used in this research contains (88.8% Al, 6% Si, 4.5% Cu, 0.5% Mg and 0.2% Sn) this type of alloys is used to make some of automotive parts such as clutch housing, pistons and sliders.

1271
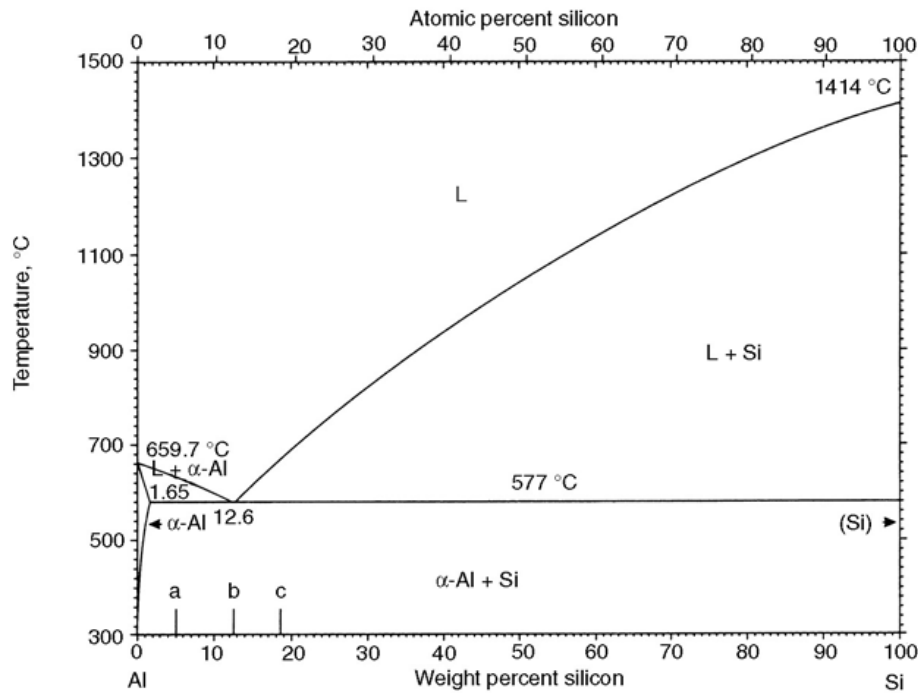
Fig. (3): Al-Si equilibrium diagram [10].

3. Predictive Maintenance:

Predictive maintenance attempts to detect the onset of a degradation mechanism with the goal of correcting that degradation prior to significant deterioration in the component or equipment based on the severity of the condition and the consequence of failure, it possible to determine an appropriate priority and course of action to minimize the risk and consequence of the pending failure [15]. The diagnostic capabilities of predictive maintenance technologies have increased in recent years with advances made in sensor technologies. A comprehensive predictive maintenance management program uses the most cost effective tools (e.g., Vibration Monitoring, Thermograph, Tribology) to obtain the actual operating condition of critical plant systems and based on this actual data schedules all maintenance activities on an as-needed basis. Including predictive maintenance in a comprehensive maintenance management program optimizes the availability of process machinery and greatly reduces the cost of maintenance. It also improves the product quality, productivity, and profitability of manufacturing and production plants.

There are three basic techniques of predictive maintenance:
1. Existing sensor – based maintenance techniques.
2. Test sensor – based maintenance techniques.
3. Test signal-based maintenance techniques.

The first one consists of maintenance methods that use data from existing process sensors such as pressure sensors, thermocouples, and resistance temperature detectors that measure variables like temperature, pressure, level, and flow. The second uses data from test sensors such as accelerometers for measuring vibration and acoustic sensors for detecting crack initiations of materials or other sound sources for failures caused these sounds such as leaks in vessels. The third one represents the active techniques while the previous are passive techniques. One form of test signal–based predictive maintenance involves injecting a signal into the equipment to measure their performance [7]. A significant amount of work has been done by NASA to measure the range when journal bearings emit ultra-sonic noise when wear has developed [3].

4. Experimental:
4.1 Specimens Preparation:

Specimens in this research are prepared by powder metallurgy. Powder metallurgy provides porosity with homogeneously distribution. The powder which have been used for making the specimens pressed at (100, 200 and 600) MPa to make a variety of porosity volume percentages and porosity percentage for the load subjected surface area. A Lico wax C used as a pressing lubricant and the specimens sintered in a tube furnace in the presence of Nitrogen gas at 560°C for 20 minutes then slow cooled to 480°C. The difference compaction pressures make samples with variable densities.

The green and sintered densities of samples were determined according to Metal Powder Industries Federation standard. The un-sintered (green) density of the samples was calculated for each sample by weighing the samples in air (W**air**) and in water (W**water**). The green density calculated using eq. (1)

$$\rho_{Green} = \frac{W_{air} * \rho_{water}}{W_{air} - W_{water}} \qquad (1)$$

The temperature of the water was 20.6°C while the temperature of specimens about 20° C. The sintered density was performed by weighing the samples in air (W_{air}) prior to infiltrating them with ESSO-NUTO H46 hydraulic oil then weighing the samples in air (with oil impregnation) then measuring weight of the samples which are impregnated by the oil in the water. Finally the sintered density is calculated by eq. (2)

$$\rho_{sintered} = \frac{W_{air} * \rho_{water}}{W_{ao} - W_{wo}} \qquad (2)$$

The volume percentage of porosity is calculated using eq. (3)

$$P_V = 100 - \left(\frac{sintered\ density}{theoritical\ density} * 100 \right) \qquad (3)$$

The results of volume percentage of porosity are shown it table 1

Table (1) green and sintered density values

Specimen	Green Density (g/cm³)	Sintered Density (g/cm³)
Pressed at 100 MPa	2.13	2.3
Pressed at 200 MPa	2.3	2.47
Pressed at 600 MPa	2.57	2.59

The theoretical density of the alloy calculated to be 2.75 (g/cm³) according to the rule of mixture.

4.2 Hardness Test:

The difference of compaction pressures for the specimens gives them a different hardness. Measuring hardness of the specimens before preparation have been made, because the image analysis of the specimens requires high quality surface, destructive method of hardness test (Rockwell Hardness Test) have been used. The tool used was a diamond cone with a 60 kg load. Twelve measurements at twelve different places were taken for each sample to insure that any irregularities in the surface can't affect the hardness value. The total penetration depth is consisted of a plastic component and an elastic recovery component which have been evolved during the period of unloading. The hardness values of the specimens are (34, 49 and 58) HRA for the specimens (100, 200 and 600) MPa.

Zouhair I. Ahmed
Ameer Hussein Ali
Soroor K.Hussain

4.3 Preparation for Image Analysis:

First of all, each specimen has been divided into three sub-specimens because nine specimens are needed in this work, and then put them again into a furnace to evaporate the oil which used during cutting them. The specimen surface should be prepared very well with less possible number of scratches. The reason of that, is to get an accurate determination of the surface porosity percentage, and then each specimen is grounded by using 240, 320, 400 and 600 grit SiC abrasive papers then polished by using a billiard pad cloth, which is suitable for Aluminium Silicon polishing, with water contained of (1, 0.3 and 0.05) µm grains of Gamma Alumina powder. After polishing, the specimens have been washed properly and put in a cup of water in an ultrasonic device to remove the residual grains of polishing powder then the sample was subjected to a hot air to drying them. The measured surface roughness for the specimens (100, 200 and 600) MPa around (1.40, 1.34 and 1.28)µm respectively.

4.4 The Image Analysis:

The purpose for image analysis is to calculate the surface porosities by using the software Image Pro Plus. In this research, the Metallurgical Microscope BX51 equipped with bright-field objectives have been used to take images at high resolution. According to the ASTM (E 1245) standard test, 36 images have been taken for each sample with same magnification equal to 100x such as the pictures in figure (22). Porosities have been identified based on the variation of their grey-level intensity compared to the matrix. Grey-level threshold settings were selected to allow autonomous detection of porosity using the "flicker method" of switching back and forth between porosity and the matrix. The grey-level thresholds in addition to boundary conditions such as(aspect ratio, minimum radius and area) were set to avoid second phase particles and dendrites detection Counting method has been chosen to correct the edge effects, so the porosity lying across the boundary field is counted only once. For each field the area fraction of the detected area of porosity was measured by dividing the detected area of porosity by the area of the measurement field. The results of percentage of porosity surface area are (7.21± 0.156, 4.6 ± .0133 and 3.2± .011) for (100, 200 and 600) MPa respectively.

4.5 Application of The Loads:

The loads have been applied by using the UMT according to ASTM (G 133-5) 2010. Dry, reciprocating test is done by utilizing the upper ball specimen which slides against a flat lower specimen in a linear, back and forth, sliding motion having a stroke length of 5.03 mm. All the tests have been applied at room temperature and relative humidity of 40-55%. The load has been subjected downward through the ball contour-face against a flat specimen mounted on a reciprocating drive. The tester allows for monitoring the dynamic normal load, friction force and depth of the wear track during the test. The weight of the specimen was measured before and after each wear test to determine individual weight loss at selected time intervals. Three different loads of (1000, 1500 and 2000) g have been subjected to 10 Hz frequency or velocity (100.6 mm/s) and three different time intervals (10, 45 and 90) minutes. After wear tests, the worn surfaces and cross sections of wear tracks are examined using Scanning Electron Microscope.

5. Results:

The results monitored by the Universal Material Tester machine which is used for testing the specimens which have been discussed. The weight loss, wear rate, coefficient of friction, wear track depth and acoustic emission sensor results have been monitored for wear test of the specimens.

5.1 Effect of Applied Load:

Weight loss increases by increasing of the applied load due to high stresses leading to the yielding and subsequent fragmentations and oxidation during sliding, the applied load also causes the strain hardening for the metals depends on the property of the metal which is under the load [8,6,5]. In the fig. 4 (a, b and c) weight loss raised for the specimen 100MPa from 1.9mg at the load 1000g and 60.36m sliding distance to 3.6mg at the load 2000g with same sliding distance this increasing occurred for all the specimens but with different ratios depend on the load and the

porosity volume for the specimen. Wear rate will increase as a result of the increasing of weight loss for example the specimen of 600MPa compaction got increasing in wear rate from (0.00883 to 0.01472)mg/m for the load 1000g and 2000g respectively and at period 90min.

5.2 Effect of Porosity:

The presence of porosity clearly effects on the abrasive wear and other wear mechanisms due to the role of pore with its capacity to catch the fragments or debris of the worn surfaces. The filling of pores by the debris or oxides will improve wear resistance for the material according to prevent oxides debris to take the role of abrasives also it'll prevent the detachment of pores edges. Pores will reduce the micro contact between the two mating surfaces which is leading to reduce the friction and the wear. Shape of pore plays a significant role in filling the pore by the debris also in term of crack initiations and stress concentration the circular shape it's the best one because it's easier to fill and the less in term of stress concentration [14].

In fig. 5 (a, b and c) the wear rate decreases markedly during the increasing of sliding distance specially at load 1000g for the highest porosity volume which is the specimen 100MPa also at load 1500g, the value of wear rate at the 540.24m of sliding is convergent in spite of the difference by hardness values. At load 2000g the effect of the porosity lowered in term of wear rate improvement due to the lower magnitude of hardness for a specimen which has high porosity volume percentage. In addition to that the scanning electron microscope images for debris of this load show big size for debris of worn surfaces at load 2000g consequently big size of debris with small pores lower the probability of entrapping the debris in pores so the debris of worn surface and oxide of Al would be as abrasives for the surface in addition to the applied load.

5.3 Coefficient of Friction:

Coefficient of friction increases by increasing the applied force but it's also affects by the geometry of the surfaces [20]. Surface has complex effect on COF due to the valleys and grains orientation [4]. Friction causes energy dissipation as heating leading to softening of the metal and thermal oxidation of the surface. Aluminium oxide is has high hardness and so adhesive to the surface so it will need high load to penetrate [12]. Figures In this research the surface finish for the specimens is treated to be good for reducing the effect of surface roughness. Pores presence will increase surface roughness specially the big sizes but when debris settle down in the pores COF will decrease or get more stable [11]. All the specimens in this research COF got slight increasing by increasing the load but specimens of 100MPa compaction got more COF increasing than other due to lower hardness so it's easy to penetrate. the specimen 100MPa with load 1000g COF decreased to the half in addition to lower wear track depth while that didn't appear with other loads because 1500g and 2000g overcame the presence of the oxide layer and strain hardening for the specimens. COF trends for the specimens of 200MPa are stable but with clear increasing for loads 1500g and 2000g due to detachment of the oxide layer which causes adhesion with the tool and surface as observed by naked eye exam for the tool and SEM for the wear track. Specimens of 600MPa compaction high hardness with the oxide layer give the stability for COF trends except for the load 2000g a slight increasing was observed.

5.4 AE Results:

The sources of AE sensor of sliding test come from plastic deformation, initiation and growth of cracks, appearance of wear debris, of new surfaces because of wear and energy liberation at repeated deformation or phase hardening-weakening and damage of surface layer. Characteristics of AE are sensitive to the wear mode. Higher AE intensity values are typical with abrasive wear in comparison with adhesive and fatigue wear.

When studying the shape of AE signals at steady-state friction it was found that materials damaged by adhesion and fatigue produced a continuous signal with a small amplitude while materials damaged by adhesion with seizure yield a signal of explosive type. When the abrasive wear becomes dominate the amplitude of signals increase approximately 2–3 times [21]. Specimens which are compacted under 100MPa have lowest AE intensity with continues stability and little amplitudes relatively to the others as shown in Fig. (9). According to the trends of 200MPa and 600MPa specimens, AE intensity is relatively high and abrasive wear appeared more effective than adhesive, also it is easier to detach the surface of lower compaction metal due to it has relatively low hardness.

5.5 Wear Track Depth:

The figures give same trend which is the increasing of depth value by increasing the applied load. In addition to that, the monitoring process for the test shows the changes of depth's value during the test and the differences among specimens. In figure (10 a) the changes in the trend is less than of figure (10 b), this is because the specimen 100MPa has more pores than 200MPa and its pores are bigger in the size. The changes in trend of figure (10 c) is less than of figure (10 b), here the effect of hardness takes part to make the test value seems more stable. There is another explanation for depth trend changes caused by the porosity, where debris of worn surfaces for a specimen which has high number and big size of pores has no effect on the depth trend such as the specimen which has less number and smaller size of pores, will be between the two contacting surfaces so debris reduces the depth then it will increase the value of the depth when debris leave away the contact area. SEM images show the size of debris at load 2000g and load 1000g. At 2000g size the debris is bigger than at 1000g; this prevents pores to be contained, so changes in trend of depth have been noticed. The depth value of specimen 100MPa at period 90 min is less than of the specimen 200MPa at the same period of

time; this is because of small size of debris which enables the pores to entrap it.

5.6 Scanning Electron Microscope Images:

Fig. (13 a, b, c and d) shows the drift of metal at the edge of wear track for each specimen also the detached particles which migrated due to adhesive wear or penetrated the surface by the applied pressure and surface softening as a result of frictional heat. Figure 14 (a, b, and c) shows the worn surface under 1000g and 90min, surface damage of the specimens is clear for 200MPa and 600MPa but it isn't for one of 100MPa specimens because of the role of porosity. Pores effect is not enough to reduce damage of the surface for higher loads. Surface damage for the worn surface by load 1500g appears in figure (16 a) which reveals micro cracks nearby pores in spite of filling by debris while other images of other specimens for the same conditions depict less surface damage due to their high hardness. Same thing repeated with the load 2000g the specimens which are compacted by high pressure resisted and have more wear than others but they got more damage than specimens which are subjected to load of 1000g as shown in figure (15) and (17). Higher magnification of SEM images in figure (5.30) enables us to see the effect of pore size and shape. For 100MPa the pore is large and contains large debris size in addition to small size of debris while for 200MPa pore is relatively small and contains small size debris. Figure (5.30 c) clarifies the effect of pore shape, that pore has sharp edges which are considered as stress concentrations and the place of crack initiations.
Figure (5.31) shows the effect of delamination for some grooves of 90min period, this period has a highest number of cycles so delamination occurred for this period more than others. The cracks extended from the pores under the groove to the surface have been observed. Also it's observed that specimens of 100MPa are affected by delamination more than the others.
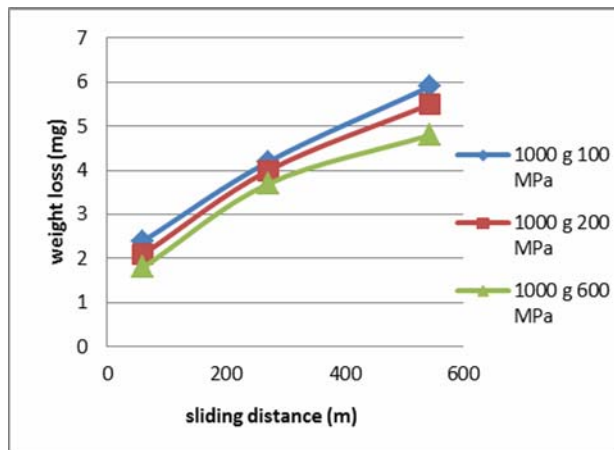
a
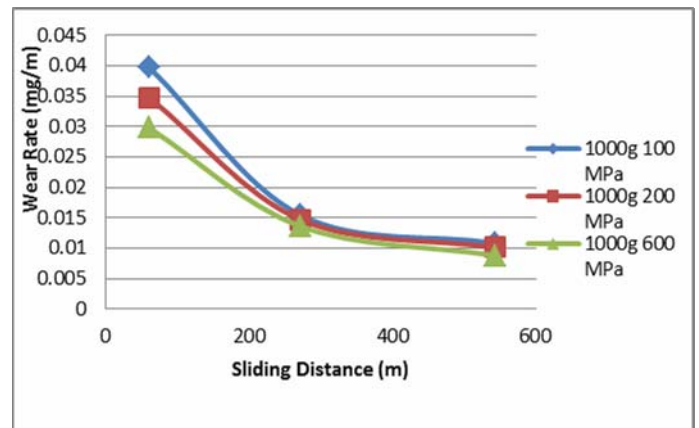
a
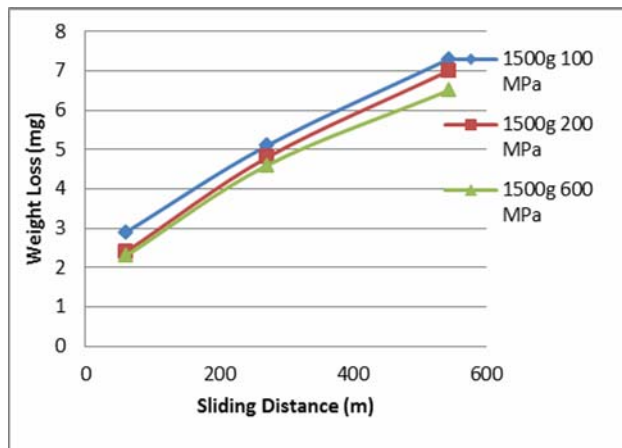
b
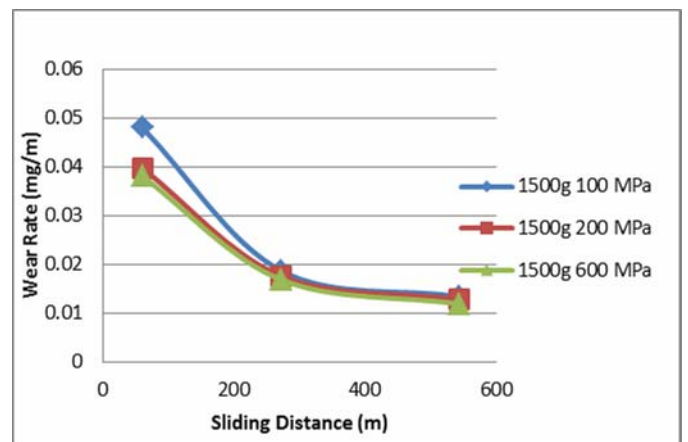
b)
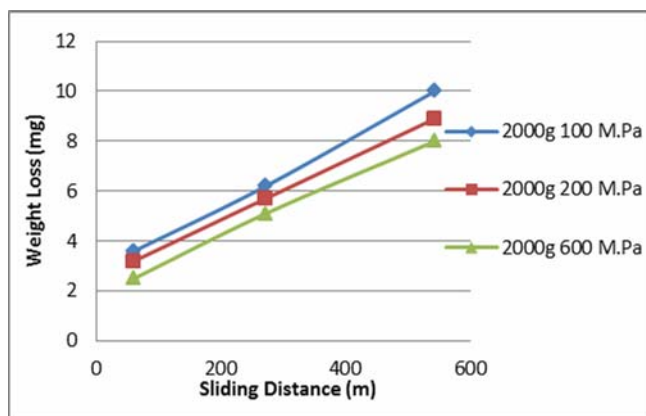
c
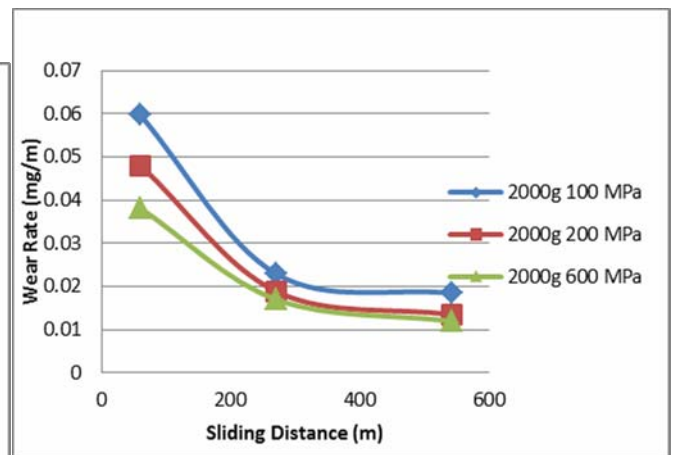
c)

Fig. (4) Weight loss vs. sliding distance for the three loads and three types of compaction (a, b and c)

Fig. (5) Wear rate vs. sliding distance for the three loads and three types of compaction (a, b and c)
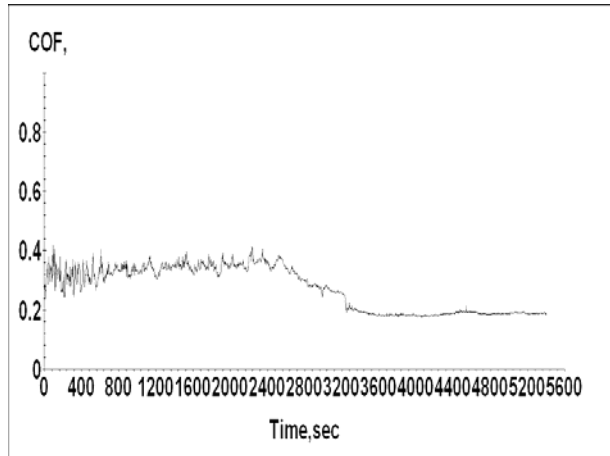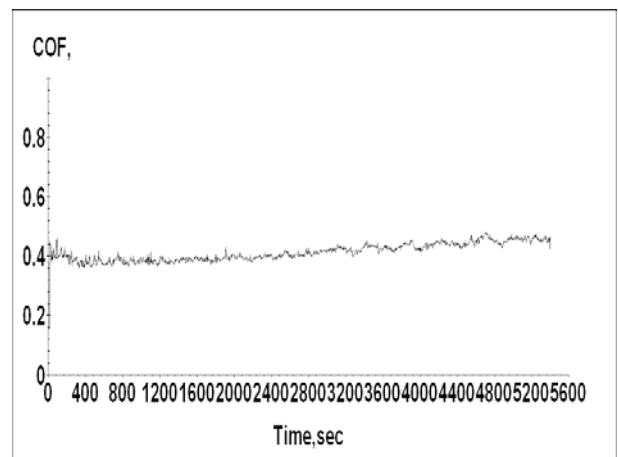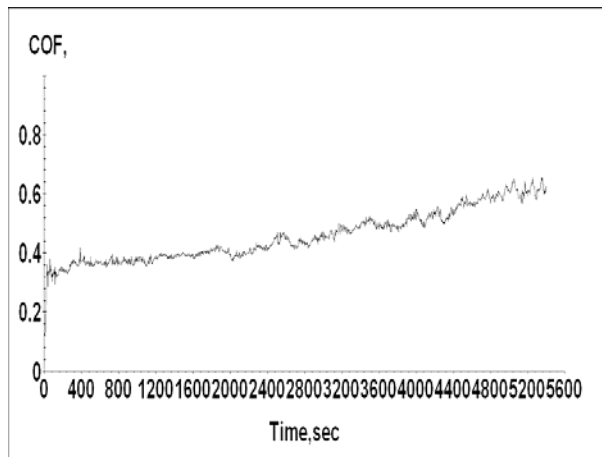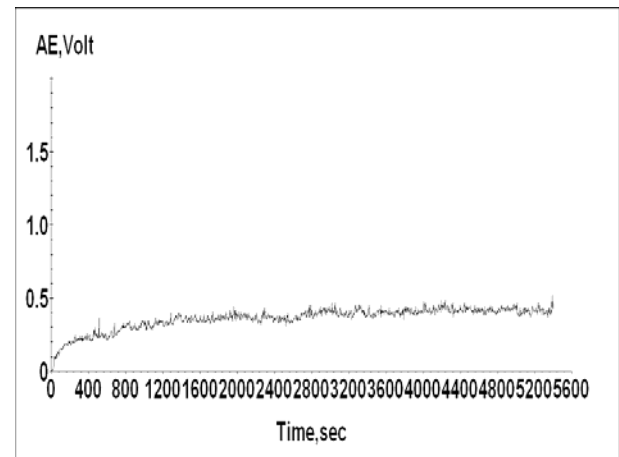
a
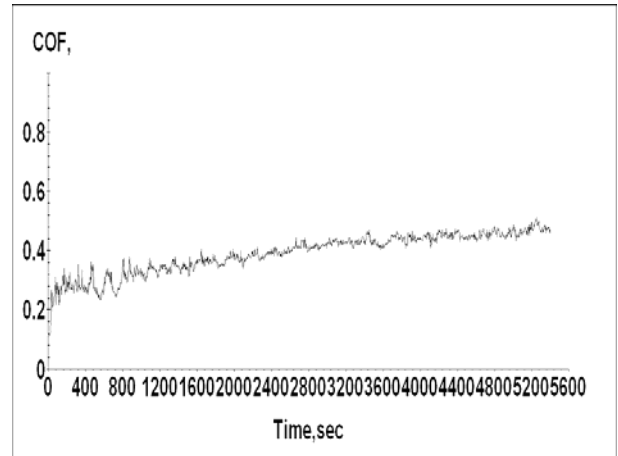
a
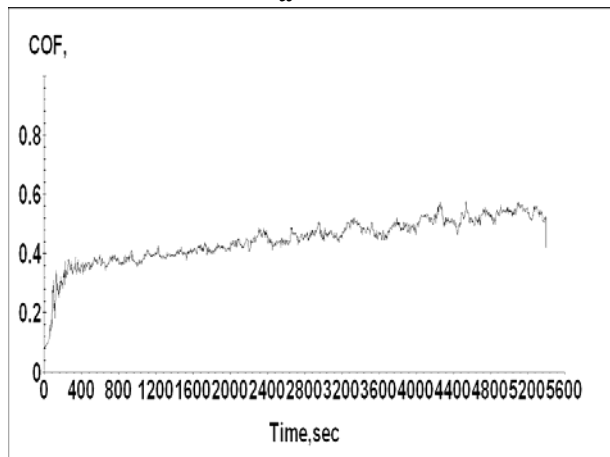
b
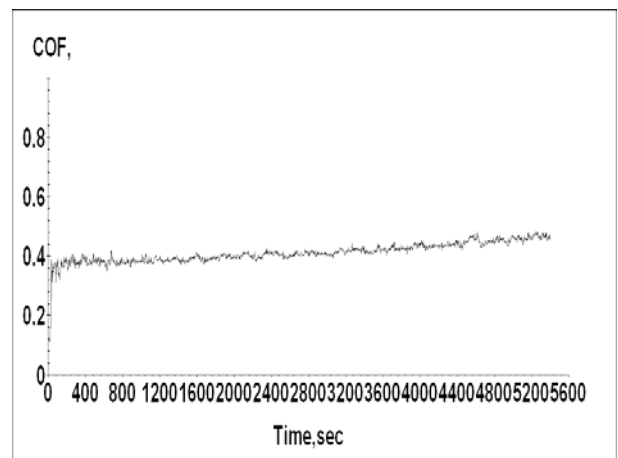
b
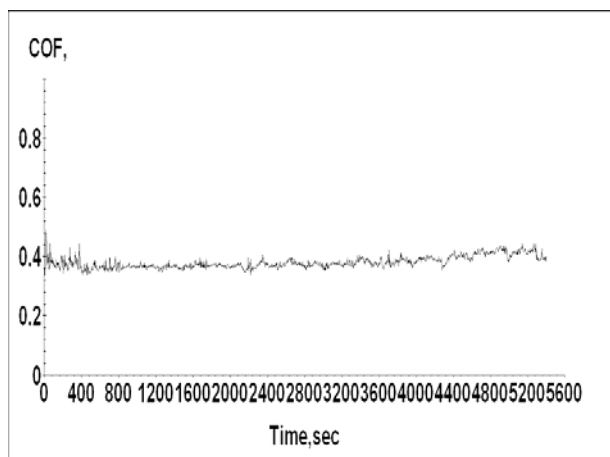
c

c

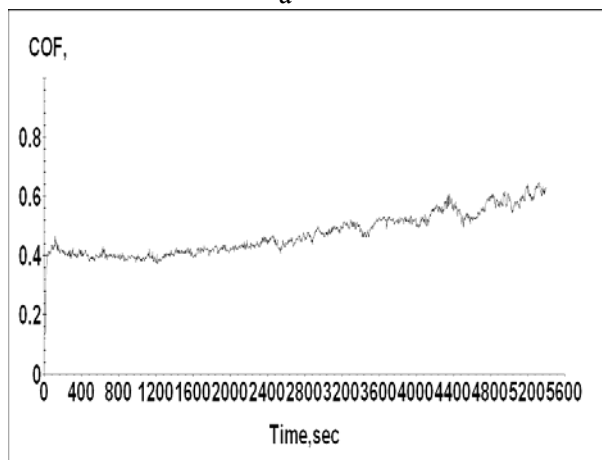**Fig. (6)** COF 1000g 90 min (100, 200 and 600) MPa (a, b and c) respectively.

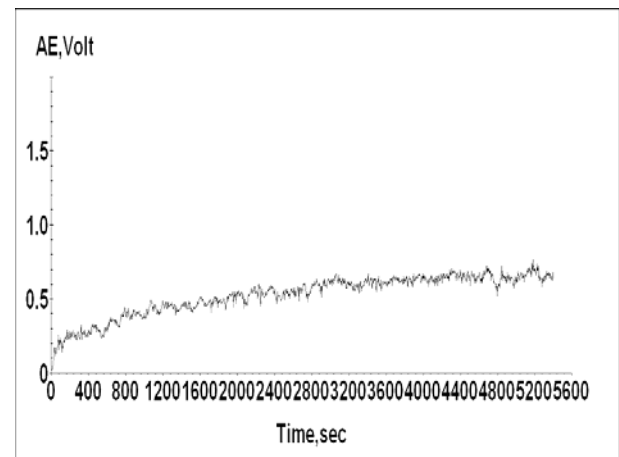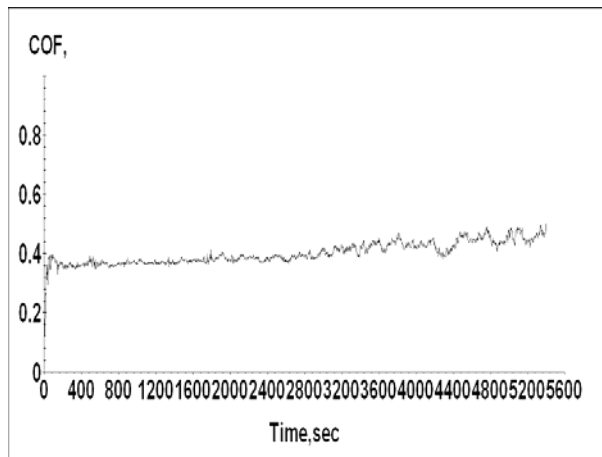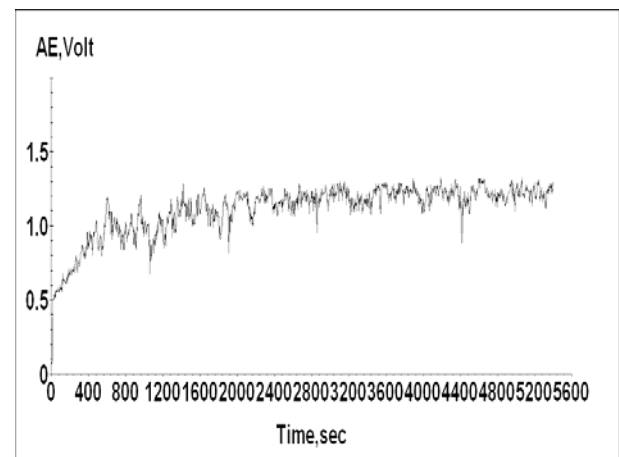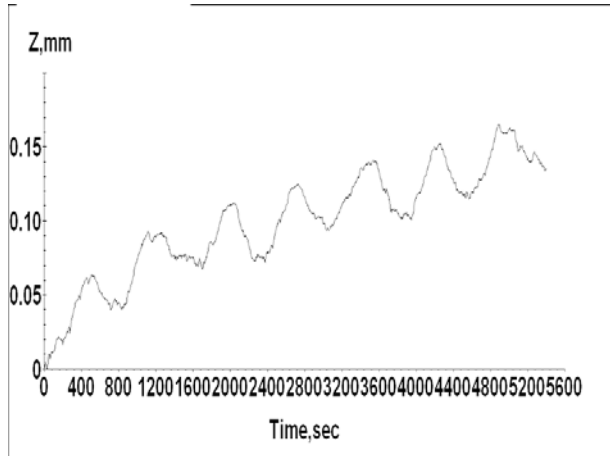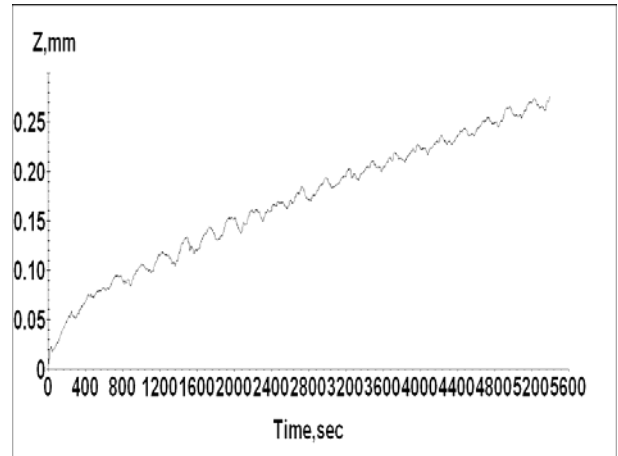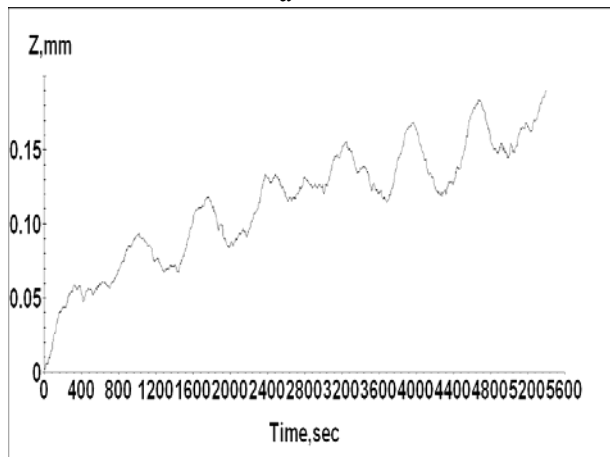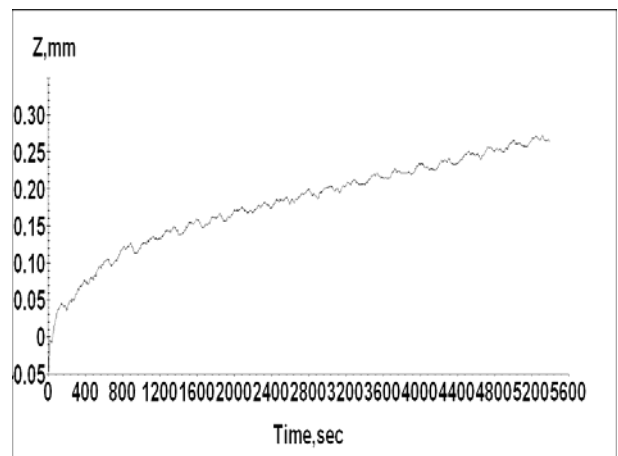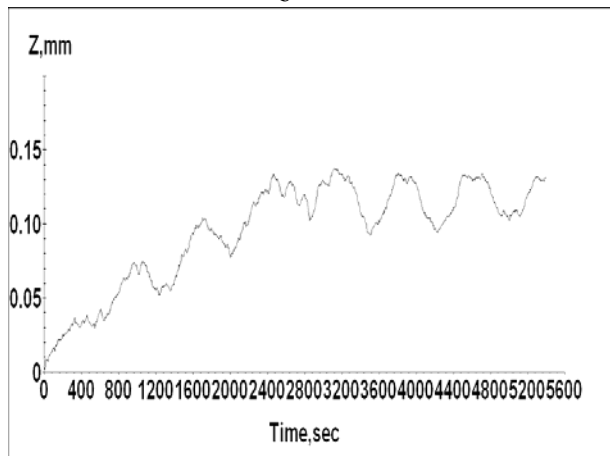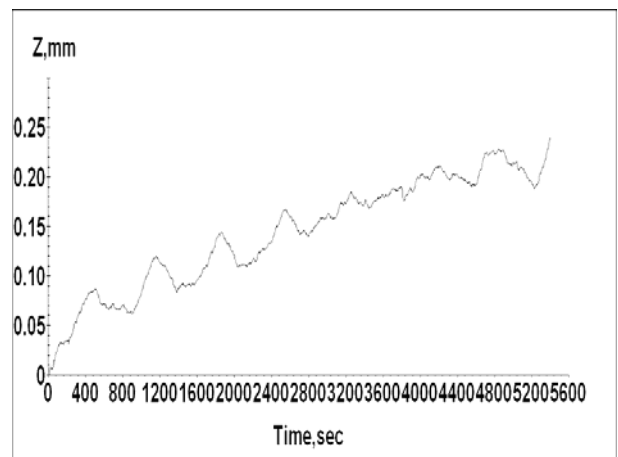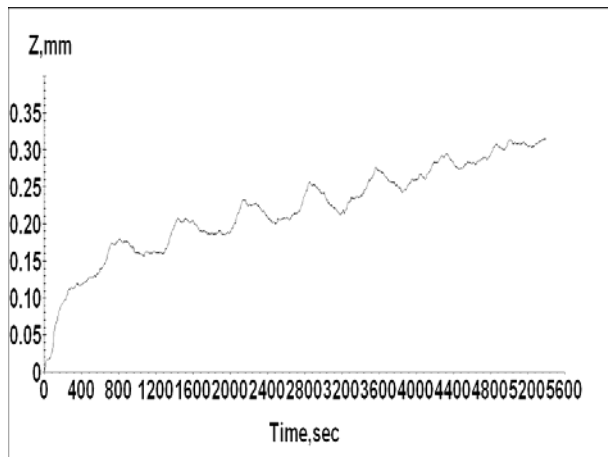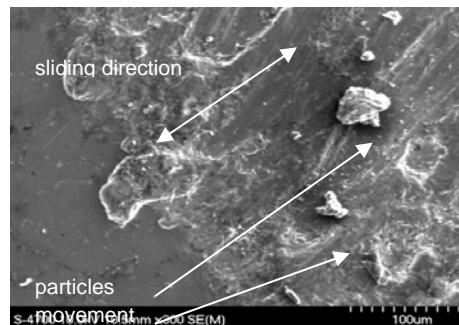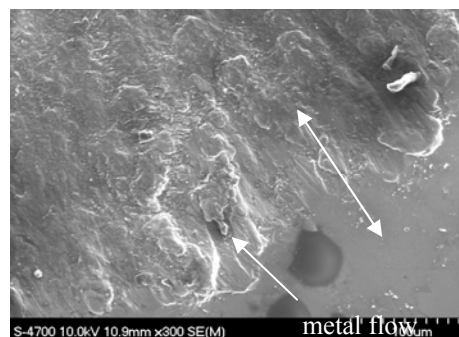**Fig. (7)** COF 1500g 90 min (100, 200 and 600) MPa (a, b and c) respectively.

Fig.(8) COF 2000g 90 min (100, 200 and 600)
MPa (a, b and c) respectively.

Fig. (9) AE 1500g 90 min (100, 200 and 600)
MPa (a, b and c) respectively.

a

b

c

Fig. (10) Wear track depth 1000g 90 min (100, 200 and 600) MPa (a, b and c) respectively.

a

b

c

Fig. (11) Wear track depth 1500g 90 min (100, 200 and 600) MPa (a, b and c) respectively.

a

a)   100 MPa 1000g 10 min

b

b)   200 MPa 1000g 10 min

c
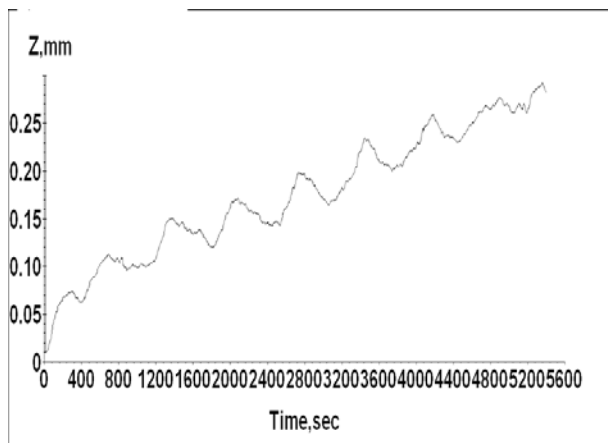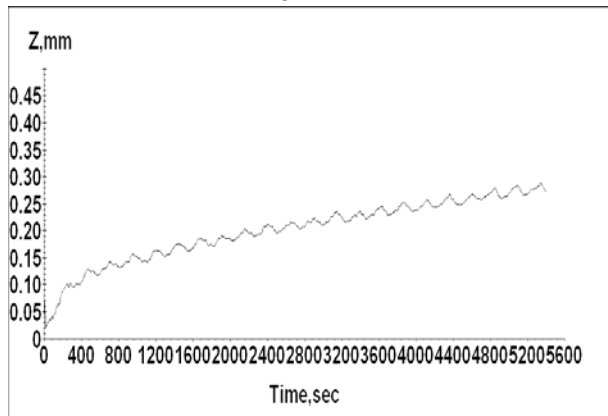
c)   600 MPa 1000g 10 min

Fig. (12) Wear track depth 2000g 90 min (100, 200 and 600) MPa (a, b and c) respectively.

d)   100 MPa 1000g 90 min

Fig. 13 (a, b, c and d) edge of the wear track.

a)

pore filled by
debris

a)

surface
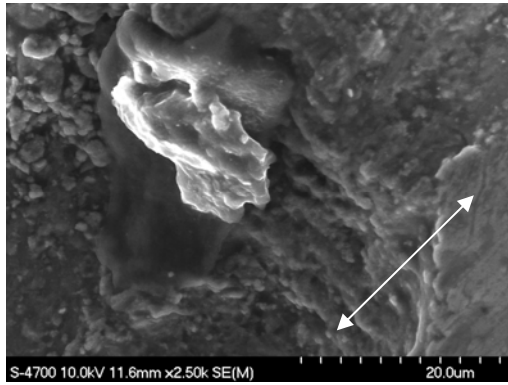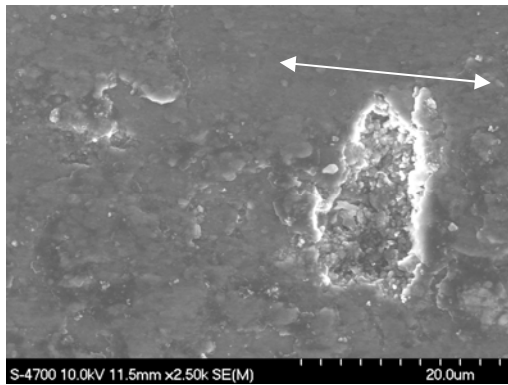damage

b)

b)

surface
damage

c)
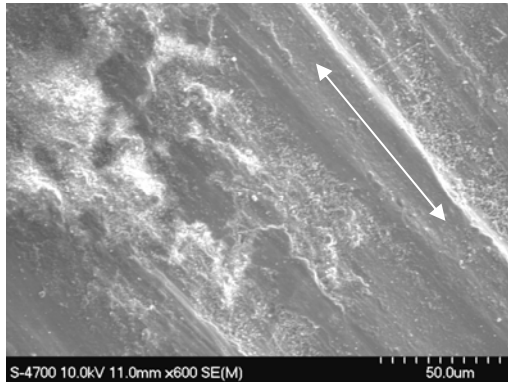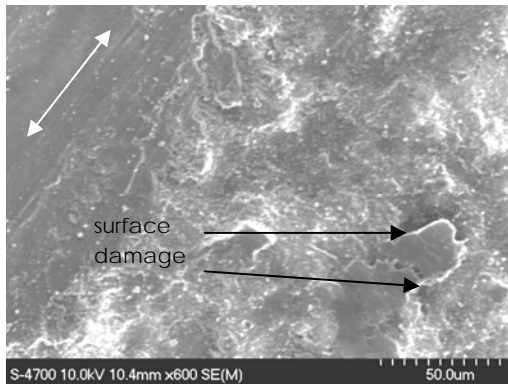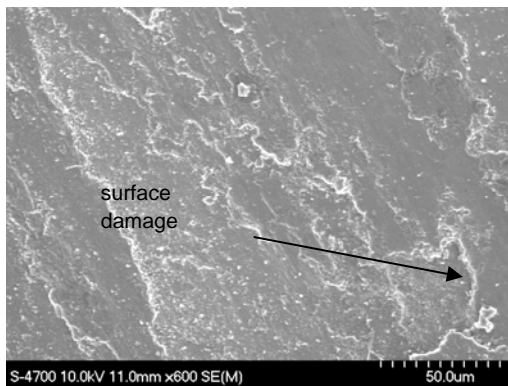
c)

Fig. (14) Wear track of 1000g after 90min for
(100, 200 and 600)MPa. (a, b and c) respectively.
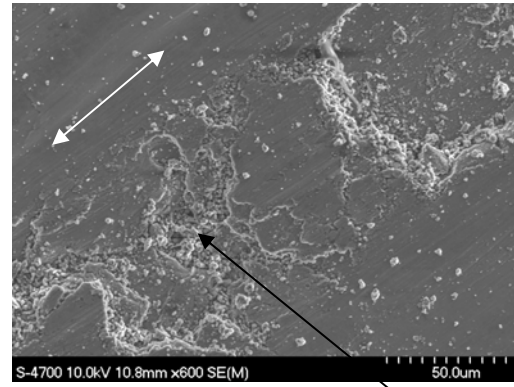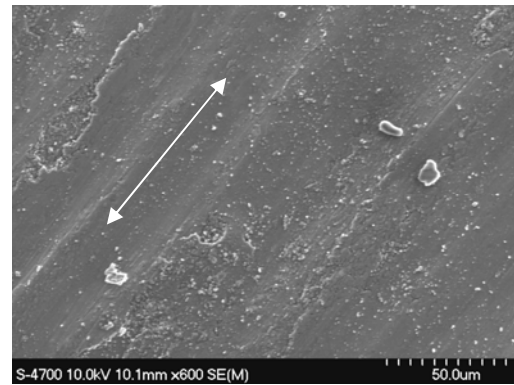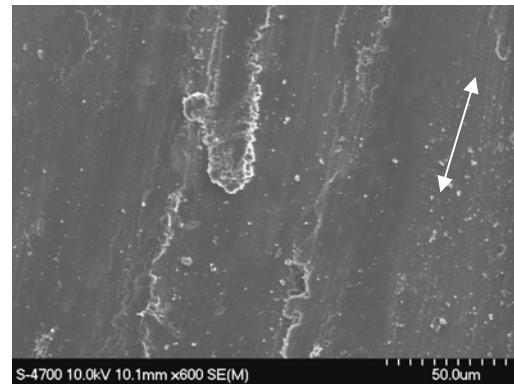
Fig. (15) Wear track of 1500g after 45min for (100,
200 and 600) MPa. a, b and c respectively.
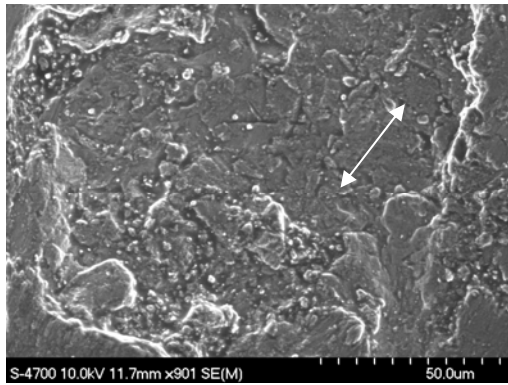
a)
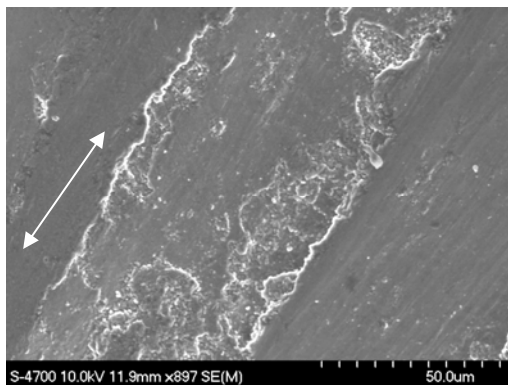
b)
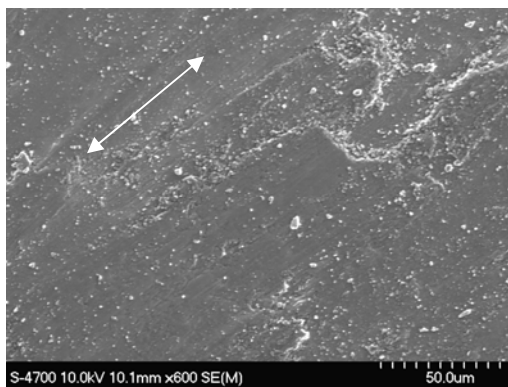
c)

Fig. (16) Wear track of 2000g after 45min for (100, 200 and 200 and 600) MPa (a, b and c respectively).
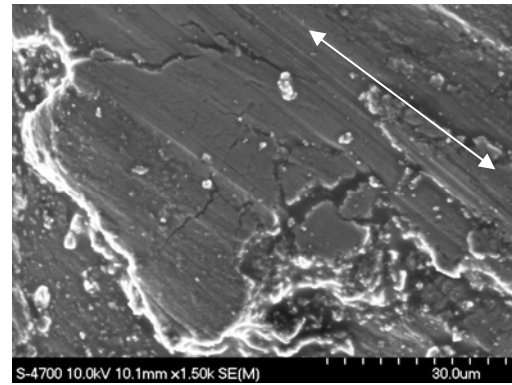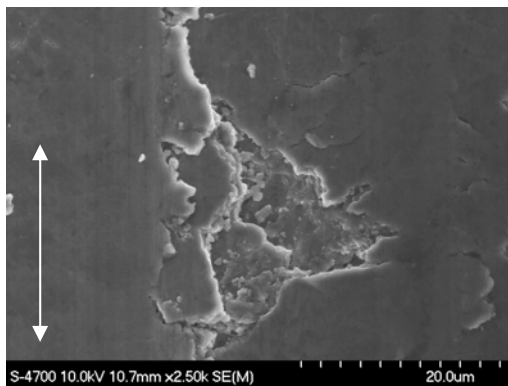

a)
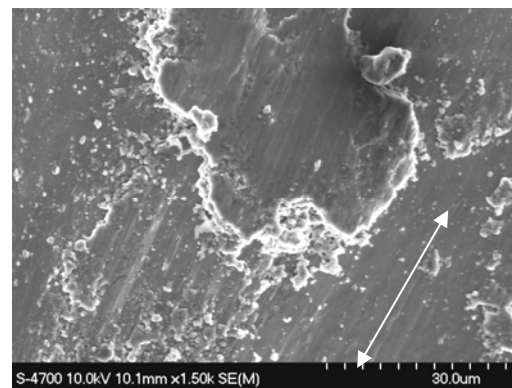
b)
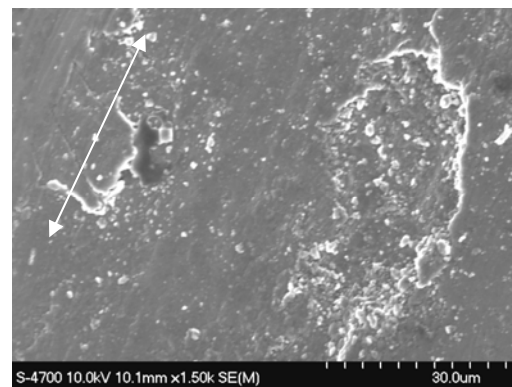
c)

Fig. (17) Wear track of 2000g after 90min for (100, 200 and 600) MPa (a, b and c respectively).
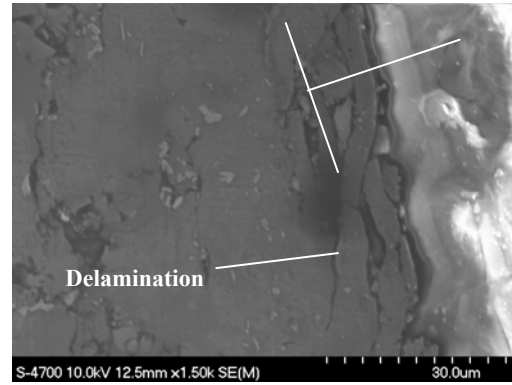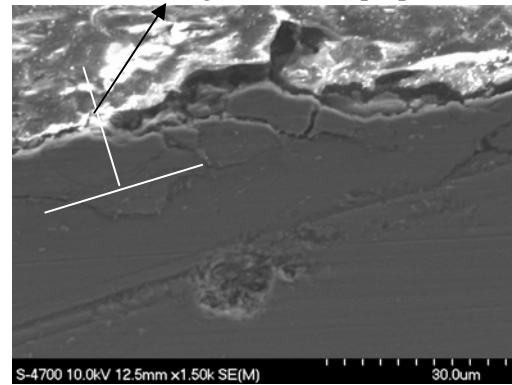
a)

b)

c)

Fig. (18) Wear track of 1000g after 90min for (100, 200 and 600)MPa (a, b and c) respectively.
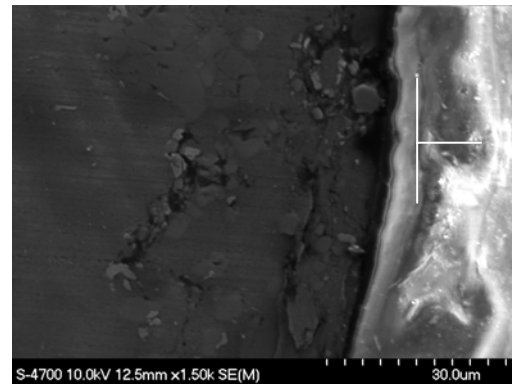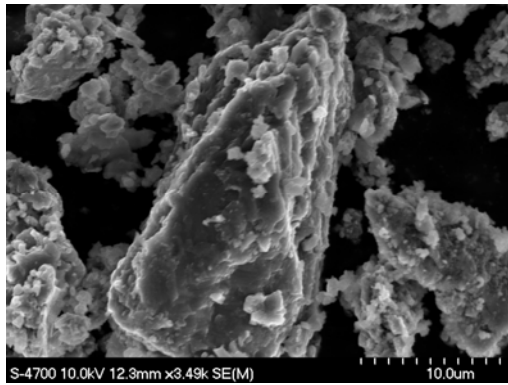
a)

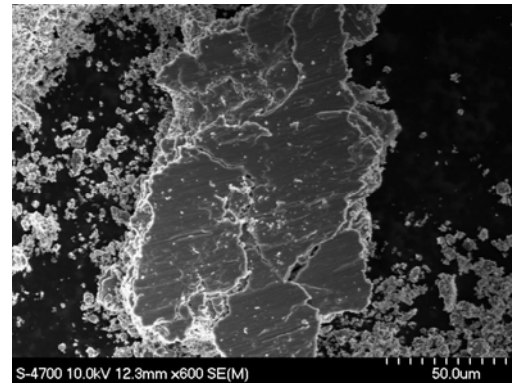Siding direction is perpendicular to the specimen
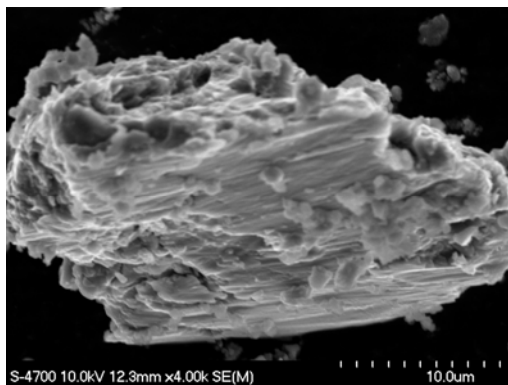
b)

c)

Fig. (19) Cross sectional image of 2000g 90min for (100, 200 and 600)MPa (a, b and c) respectively.
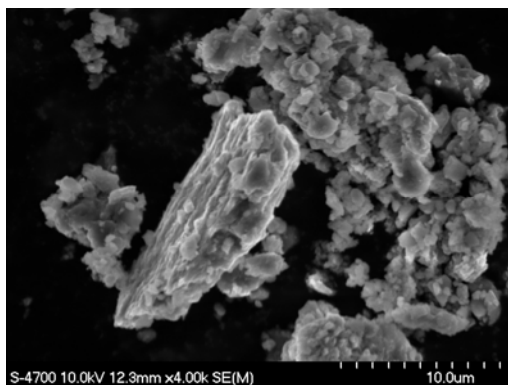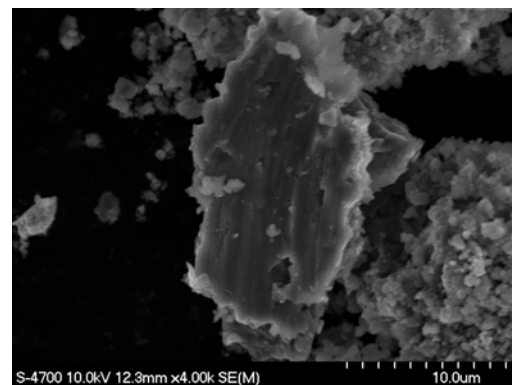
a)

b)
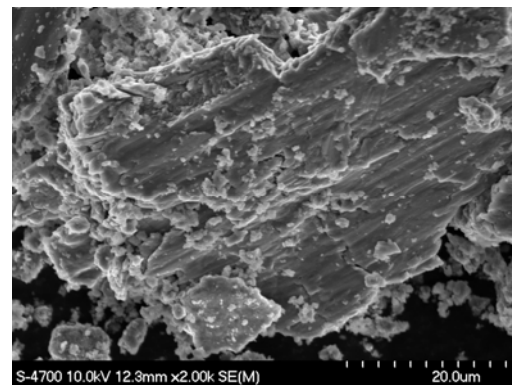
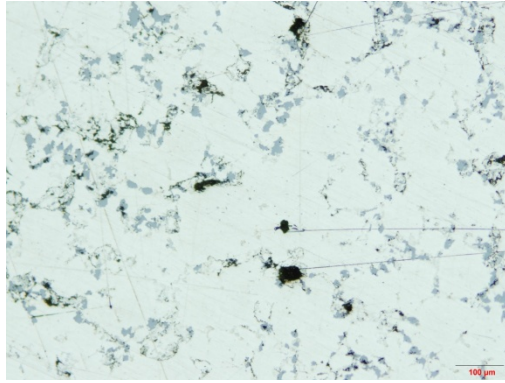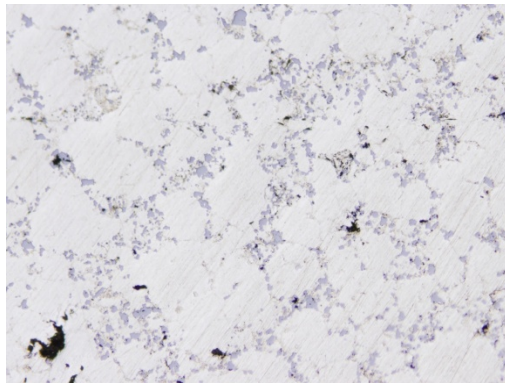
c)

Fig. (20) Debris of the specimens under 1000g for 90min (100, 200 and 600)MPa (a, b and c) respectively.
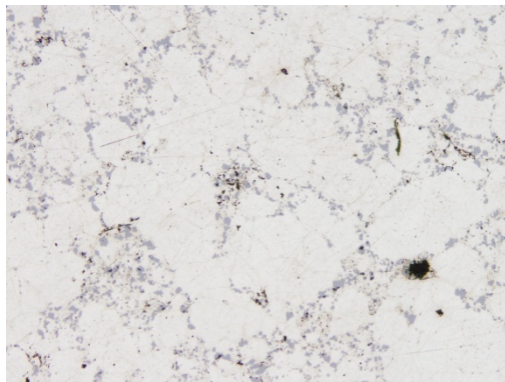

a)

b)

c)

Fig (21): Debris of the specimens under 2000g for 90min.

a

b

c

Fig. (22) Pictures for image analysis to measure

the porosity surface area percentage for (100, 200

and 600)MPa (a, b and c) respectively.

Conclusions:

1. Wear test has a dynamic environment represented by strain hardening of the surface metal after load application, softening due to heat generation because of friction; friction changes as a result of roughness changes in addition to pores presence in this research so on line monitoring results give a clear picture about wear test and its dynamic changes.

2. Porosity has a significant effect on wear resistance this appeared clearly from the results of the test. Pore size and shape play the role of porosity effect, porous surface with a relatively big size pores has better wear resistance if the applied load is low but it has worse if the load is high.

3. Agent technology has the flexibility to monitor such a dynamic environment like a dry sliding wear test and give a brief report to the individual events during the test.

4. AE results can be transferred to detect faults for any product made by the tested material depending on the similarity of test conditions because it represents on material properties and the media of sound transfer.
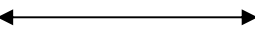
References:

1. Abdulhaq A. Hamid, S.C. Jain, P.K. Ghosh, and Subrata Ray "Characterization and Tribological Behavior of Cast In-Situ Al (Mg,Mo)-Al2O3 (MoO3) Composite", Metallurgical and Materials Transaction B, Vol. 37, No. 4, pp. 519-529, (2006).

2. A.S. Anasyida, A.R. Daud, M.J. Ghazali "Dry Sliding Wear Behaviour of Al–12Si–4Mg alloy with Cerium Addition", Materials & Design, Vol. 31, No. 1,p.p 365-374, (2010).

3. Anderson, M. L. (1994) "Predictive maintenance: its present state and future potential for the mobile equipment industries", In Proc of the Conference Equipment resource management into the 21st century, Nashville, Tennessee, ASCE, New York. 210 p.

4. B. Bhushan "Introduction to Tribology", Wiley N.Y. (2002).

5. B. Dubrujeaud , M. Vardavoulias and M. Jeandin, "The role of

porosity in the dry sliding wear of a sintered ferrous alloy", journal of wear, Vol. 174, Issues 1-2, pp.155-161, (1994).

6. B.K. Prasad, "Influence of Some Test Parameters on Dry Sliding Wear Characteristics of a Zinc-11.5% Aluminium Alloy", Journal of Materials Engineering and Performance Volume, Vol. 11,No. 4, pp. 461-468, (2002).

7. Hashemian, H. M, "State-of-the-art predictive maintenance techniques", IEEE Transactions on Instrumentation and Measurement ,Vol. 60, Issue 1, pp. 226-236, (2010).

8. H.Z. Ye, D.Y. Li, and R.L. Eadie "Influences of Porosity on Mechanical and Wear Performance of Pseudoelastic TiNi-Matrix Composites", Journal of Materials Engineering and Performance, Vol. 10, No. 2, p.p 178-185,(2001).

9. Jianbo Zhang, Regtien, Paul P.L. and Korsten, Maarten " Monitoring of Dry Sliding Wear Using Fractal Analysis". In: 10th IMEKO TC10 International Conference on Technical Diagnostics, Budapest, Hungary, (2005).

10. Małgorzata Warmuzek "Aluminium-Silicon Casting Alloys Atlas of Microfractographs ", ASM, (2004).

11. M. G. GEE, E. A. ALMOND "The Affect of Surface Finish on the Sliding Wear of Alumina", Journal of Materials Science, Vol. 25, No. 1, pp. 296-310, (1990).

12. Michael F. Ashby And David R. H. Jones "Engineering Materials 1 An Introduction to their Properties and Applications", Butterworth-Heinemann, 2nd Ed., (1996).

13. Myer Kutz, "Handbook of Materials Selection", John Wiley & Sons, (2002).

14. Piao Zhong-yụ, Xu Bin-shi, Wang Hai-dou, Pu Chun-huan " Investigation of fatigue failure prediction of Fe-Cr alloy coatings under rolling contact based on acoustic emission technique", Applied Surface Science, V. 10, 1016, (2010).

15. Ron Moore, " Selecting The Right Manufacturing Improvement Tools", Elsevier, (2007).

16. V.K. Gupta, S. Ray2, O.P. Pandey, "Dry Sliding Wear Characteristics of 0.13 wt. % Carbon Steel", Materials Science-Poland, Vol. 26, No. 3, (2008).

17. Russell, S. and Norvig, P. "Artificial Intelligence: A Modern Approach", Prentice Hall Series in Artificial Intelligence. Englewood Cliffs, New Jersey, (2003).

18. Teppo Pirttioja, Antti Pakonen, Ilkka Seilonen, Aarne Halme and Kari Koskinen" Multi-Agent Based Information Access Services for Condition Monitoring in Process Automation ", 3rd International Conference on Industrial Informatics IEEE, (2005).

19. Woolderidge. M "An Introduction to Multiagent Systems", John Wiley & Sons Ltd., (2002).

20. Valentin L. Popov, "Contact Mechanics and Friction Physical Principles and Applications", Springer-Verlag Berlin Heidelberg (2010).

21. Victor Baranov, Evgeny Kudryavtsev ,Gennady Sarychev and Vladimir Schavelin, "Acoustic Emission In Friction" , Moscow State Engineering Physics Institute Kashirskoe sh. 31, Moscow, first edition, Elsevier, (2007).

List of Symbols		
Symbol	Meaning	Unit
ρ_{Green}	Green Density	g/cm³
$\rho_{sintered}$	Sintered Density	g/cm³
ρ_{water}	Water Density	g/cm³
AE	Acoustic Emission	Volt
COF	Coefficient Of Friction	
HRA	Rockwell Hardness	
W_{water}	Sample weight on water	g
W_{air}	Sample weight on air	g
W_{wo}	Sample weight on water after impregnation with oil	g
W_{ao}	Sample weight on air after impregnation with oil	g
Vs.	Versus	

*(◄──────────►) This shape always refers to the sliding direction on SEM images.